IEEE/CSC & ESAS European Superconductivity News Forum (ESNF), No. 15, January 2011
The published version of this manuscript appeared in *IEEE Transactions on Applied Superconductivity* **21**, Issue 3, 349 - 353 (2011)

Modeling the behavior of HTS terahertz RSQUIDs

Colin M Pegrum, John C Macfarlane and Jia Du

***Abstract*—In previous work we looked in detail at simulations of our HTS Resistive DC SQUIDs (RSQUIDs) using a lumped-component model and neglecting step-edge junction capacitance. These can now be made with junctions that have a high product of critical current and normal resistance (I_cR_J) and so the Josephson frequency can be above 1 THz. This calls for a more refined model of the device, which we will present here. The RSQUID series resistor is represented as a distributed combination of resistance and inductance, rather than simply a resistor in series with its self inductance. We now include junction capacitance, as the Stewart-McCumber parameter can be close to unity. We treat the RSQUID loop as a co-planar stripline, rather than as an inductor. We report a range of simulations with these enhancements to the model and comment briefly on the results in relation to potential applications of RSQUIDs as active microwave devices.**

***Index Terms*—Superconducting microwave devices, SQUIDs, Josephson oscillators, Josephson mixers, heterodyning.**

I. Introduction and Motivation

A resistive SQUID or RSQUID is a conventional SQUID with a small resistor R_s added in series with its loop. Early RSQUIDs were RF-biased and were used for noise thermometry (*e.g.* [1]) and thermal measurements [2], [3]. Niobium thin-film versions of DC RSQUIDs [4]–[10] found similar uses. One such RSQUID [4] was used as a current-controlled oscillator in the frequency range of a few kHz to several hundred MHz. Here an external current I_s is fed through R_s to cause the average voltages across the two junctions to differ by I_sR_s. The different Josephson frequencies mix together to produce a heterodyne frequency f_h given by $f_h = (I_sR_s)/\Phi_0$, where Φ_0 is the flux quantum.

Macfarlane *et al.* [11] and Hao *et al.* [12] reported the first HTS current-controlled RSQUID oscillator, operating from 20 to 60 K at frequencies from 1 to 50 MHz and they have recently reported GHz HTS DC RSQUID oscillators [13]–[15]. We are now interested in exploring the potential of these RSQUIDs as mixers, using the internally-generated heterodyne frequency as a tunable local oscillator. Since these process and generate GHz signals, and have Josephson frequencies in the THz range, a microwave model of our RSQUID is needed. This is considered in this paper.

Manuscript received 3 August 2010. Colin Pegrum is with FieldSolutions, Glasgow G12 9SD and with the Department of Physics, University of Strathclyde, Glasgow G4 0NG, UK (e-mail: colin@fsolv.co.uk).

John Macfarlane is with the Department of Physics, University of Strathclyde, Glasgow G4 0NG, UK and with CSIRO Materials Science and Engineering, Bradfield Road, Lindfield 2070, Australia. (e-mail: j.c.macfarlane@strath.ac.uk).

Jia Du is with CSIRO Materials Science and Engineering, Bradfield Road, Lindfield 2070, Australia.(e-mail: jia.du@CSIRO.au).

II. Modeling the RSQUID

The simulation model has identical shunted Josephson junctions with critical currents I_c and shunt resistors R_J, as in Fig. 1. Equal DC bias currents $I_b/2$ are fed to each half of the RSQUID. The current I_s is fed through the series resistor R_s. I_b and I_s can be varied independently without interaction.

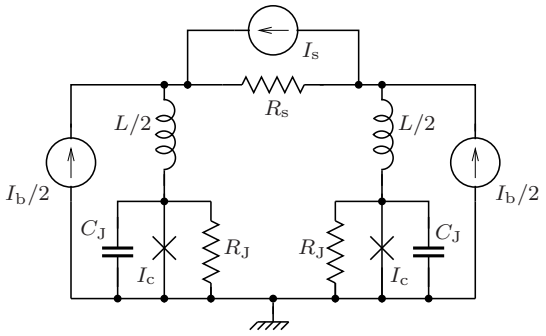

Fig. 1. RSQUID model with added junction capacitance C_J. The currents I_b and I_s are supplied by external DC sources. $R_s = 9.5\,\mathrm{m\Omega}$.

The series resistor R_s has some self inductance and ways of dealing with this are set out in Section IV. Unlike our previous analysis [16], [17], the model now includes junction capacitance C_J and the effects of this will be considered in Section V. The RSQUID loop is shown in Fig. 1 as a lumped inductance L split into two equal parts, but in Section VI we will treat it instead as a co-planar stripline (CPS). We shall conclude each of these sections with comments on new features introduced by these enhancements to the model.

For simulation we use JSIM [18], with the addition of noise sources [19] to allow the effects of a finite temperature T to be studied (though in this paper all simulations are at $T = 0$). The JSIM output is low-pass filtered and time-averaged to obtain the mean voltage $\overline{V_{out}(t)}$ for a given value of I_b, to derive the I-V curves. Statistical checks ensure the standard deviation for $\overline{V_{out}(t)}$ is acceptably small. The technique has been proven with a wide range of junction and SQUID models to confirm its accuracy [20].

III. Device Fabrication and Layout

The RSQUIDs are made from YBaCuO on MgO substrates with step-edge junctions, see Fig. 2. Full fabrication details are in [13], [14] and more recent step-edge junction improvements are in [21]. The resistor R_s is made by depositing a layer of Au over the 6 μm wide gap between the two YBaCuO tracks that are 50 μm wide. For the device modeled in this paper the tracks are 60 μm long. The series resistor is long compared with its width, to get a small value of R_s. It is $6\,\mu\mathrm{m} \times 60\,\mu\mathrm{m}$

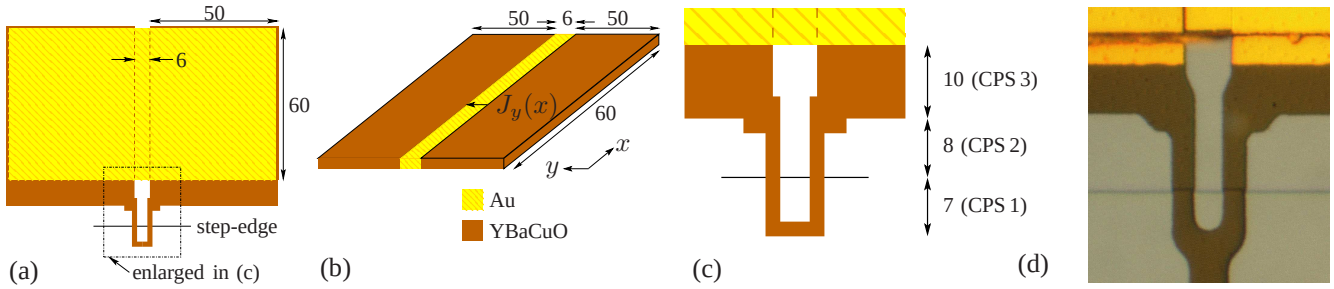

Fig. 2. RSQUID layout: (a) the complete device, (b) the effective form of the series resistor, (c) detail of the CPS part of the structure and (d) photo of the CPS section. All dimensions are in μm. The labels CPS 1, 2 and 3 relate to the CPS analysis in Section VI.

and its measured DC resistance is $9.5\,\mathrm{m}\Omega$, consistent with the separately-measured sheet resistance of the Au film at 77 K of $\approx 0.1\Omega$ per square. This confirms that the contact to the Au is predominantly at the inner edges of the YBaCuO tracks, at the dashed lines in Fig. 2(a), with negligible contact resistance. So the structure for R_s is as in Fig. 2(b)—two YBaCuO tracks with a gap filled by Au; the Au overlying the YBaCuO can be disregarded.

IV. The Series Resistor R_s

It is essential to consider the self inductance of the YBaCuO tracks that form part of R_s, since in principle this will add to the total inductance of the RSQUID loop. We have shown previously [16], [17] that RSQUID dynamics are quite strongly dependent on the total loop inductance. We have also found that the heterodyne amplitude decreases significantly as loop inductance increases [22], so stray inductance within R_s needs to be addressed and should ideally be minimised.

The impedance of the structure for R_s is not simply a series combination of resistance and inductance. This is because at high frequencies the current density $J_y(x)$ in the Au (Fig. 2(b)) varies with position x, since parts furthest away from the junctions are more isolated by the inductance of the YBaCuO lines connected to the Au. $J_y(x)$ is also frequency-dependent. This calls for a more complex model.

Some simplified options that can be used in JSIM circuits are shown in Fig. 3: rather than being a pure resistance (a) or a simple series combination of a resistor and an inductor (b), we expect it to be represented better as a distributed network of resistance and inductance, as in (c).

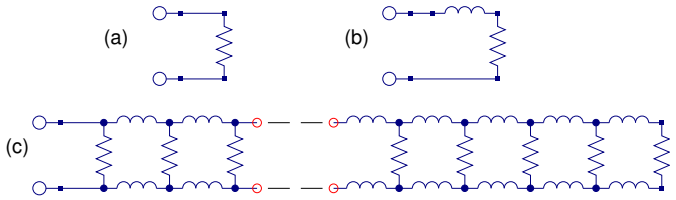

Fig. 3. Options for the equivalent circuit for the series resistor.

To analyze this we first determined the inductance per unit length of the broad YBaCuO tracks in Fig. 2(b) either side of the Au, following Chang [23] for superconducting co-planar lines. This gives $0.488\,\mathrm{pH}/\mu\mathrm{m}$, or a total inductance of 29.3 pH. Then, using the L-R ladder network in Fig. 3(c) with ten elements, we used QUCS [24] to determine the impedance $Z(f)$ of this network as a function of frequency f. This has a resistive component $R_\mathrm{s}(f)$ in series with an inductive component $L_\mathrm{s}(f)$, so that $Z(f) = R_\mathrm{s}(f) + 2\pi j f L_\mathrm{s}(f)$. $R_\mathrm{s}(f)$ and $L_\mathrm{s}(f)$ are plotted in Fig. 4.

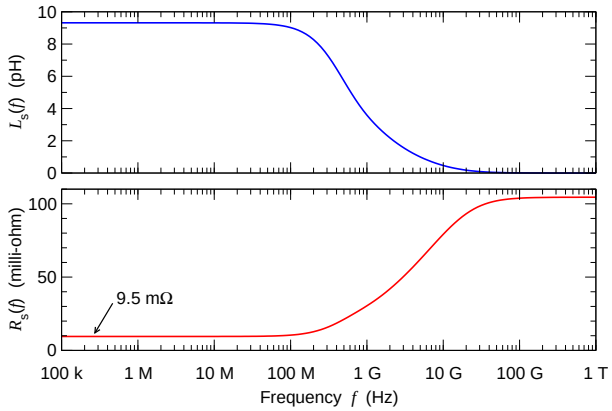

Fig. 4. The equivalent resistance $R_\mathrm{s}(f)$ and inductance $L_\mathrm{s}(f)$ for the series resistor structure.

A different analysis by Fasthenry [25] and a model made up from both superconducting and resistive films gave similar results for $Z(f)$ and also confirmed our tacit assumption that the inductance of the Au is negligible.

Fig. 4 identifies some significant issues. First, even at $f = 0$, the effective inductance is much less than 29.3 pH, simply because not all the current flows through all parts of this inductance. Next, although R_s has its DC value up to $\approx 100\,\mathrm{MHz}$, at higher frequencies $R_\mathrm{s}(f)$ increases, since then only a small part of the Au carries the current—much of the Au filling in R_s is isolated at high frequencies by the inductance of the YBaCuO tracks. Lastly, above $\approx 10\,\mathrm{GHz}$, $L_\mathrm{s}(f) \to 0$. So for currents in the RSQUID at typical Josephson frequencies, $L_\mathrm{s} \approx 0$.

To explore these issues we used JSIM to generate I-V curves for the circuit in Fig. 1, but with R_s modeled in turn as either Fig. 3(a), (b) or (c). These are shown in Fig. 5. From these and Fig. 4 we conclude the differences between the simple R-only model and the more complex L-R network are small, and fortunately for most purposes the inductive part of the series resistor structure can and should be set to zero. The $L + R$ model wrongly adds significant inductance and is substantially different and unrealistic at all voltages, so it should *not* be used.

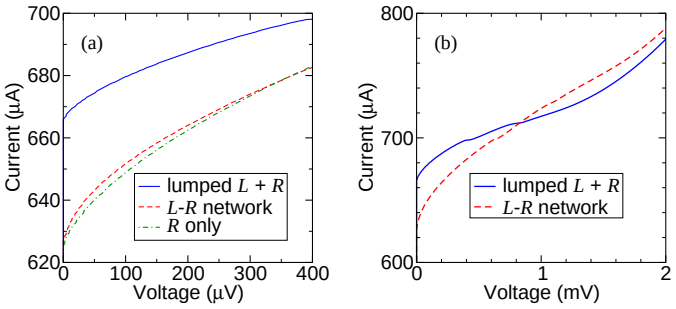

Fig. 5. I-V plots for different models for the series resistor structure. (a) At lower voltages there is a small difference between the L-R network and R-only models. (b) Above $\approx 500\,\mu$V the L-R network and R-only models are indistinguishable, so in (b) the R-only data has been omitted for clarity.

V. Junction Capacitance

Our experimental RSQUIDs [13], [14] have $2\,\mu$m-wide step-edge junctions and from [26], $C_\mathrm{J} \approx 18\,$fF. I_c is temperature-dependent and for some cooled samples rises to $250\,\mu$A; with $R_\mathrm{J} = 8\,\Omega$ the Stewart-McCumber parameter $\beta_\mathrm{C} = 2\pi I_\mathrm{c} R_\mathrm{J}^2 C_\mathrm{J}/\Phi_0 = 0.87$, so we expect junction capacitance to play a significant role in devices dynamics. Similar junctions used as detectors for THz imaging [27] have higher values of I_c and clearly show hysteresis below 20 K and also show sub-harmonic steps in their I-V curves when irradiated at 0.6 THz, which may be attributable to junction capacitance. Mitchell and Foley [28] estimated $10 < C_\mathrm{J} < 40\,$fF from the onset of hysteresis. So in what follows we set $C_\mathrm{J} = 18\,$fF.

As Section VI shows, the total capacitance of the lines in the CPS model is 2.3 fF, which is much less than C_J. So this line capacitance can be ignored at low voltage, where no transmission line resonances are excited. There is then a damped resonance between the junction capacitances $C_\mathrm{J}/2$ in series and the RSQUID loop inductance L. The CPS model (Section VI) shows that $L = 21.2\,$pH. The resulting resonance is centered on 346 GHz or $716\,\mu$V, as shown in Fig. 6 for a simplified RSQUID model.

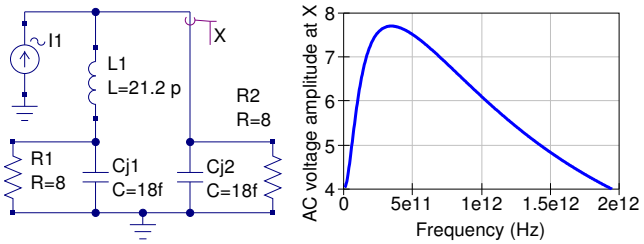

Fig. 6. Resonance of the junction capacitance C_J and loop inductance L.

Our previous JSIM modeling of an RSQUID with $C_\mathrm{J} = 0$ [16], [17] showed its I-V curve has self-induced steps due to f_h, and at $f_\mathrm{h} \approx 50\,$GHz sub-harmonic steps and other features appeared, but there was no evidence of chaos. For the present work, with $C_\mathrm{J} \neq 0$, there is a region in the I-V curve that has chaotic behavior. It extends symmetrically each side of the voltage corresponding to the damped L-$C_\mathrm{J}/2$ resonance, as Fig. 7(a) shows for $f_\mathrm{h} = 1.15\,$GHz. The width of this region is largely independent of f_h. It is associated with a peak in the amplitude of the Josephson AC voltages, seen as a peak in the heterodyne amplitude, as shown in Fig. 7(b). It is not present for $C_\mathrm{J} = 0$ and its voltage position scales as $\approx 1/\sqrt{C_\mathrm{J}}$.

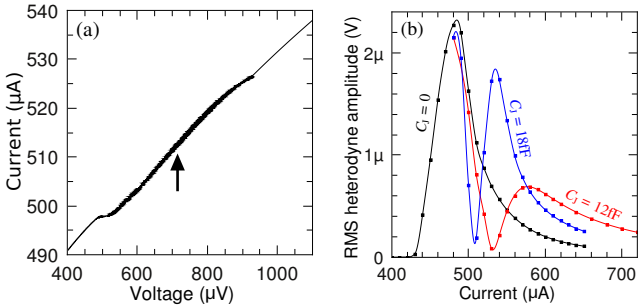

Fig. 7. The resonance in Fig. 6 introduces a chaotic region in the I-V curve centered on $716\,\mu$V (arrowed). f_h for this plot is 1.15 GHz

The equations for an RSQUID with $C_\mathrm{J} \neq 0$ are third order and so can have chaotic solutions under some conditions [29]. This is a complex system with a very rich dynamical behavior and a six-dimensional parameter space (C_J, L, R_J, R_s, I_b and I_s). Exploring it fully is beyond the scope of this paper, but Fig. 8 shows representative features of parts of I-V curves for a range of values of f_h. Fig. 8(a) shows the transition as I_b increases, from regular steps into a chaotic state, and there is clear evidence of subharmonic steps at higher f_h in Figs. 8(b)-(d). The frequencies cover those of interest for mixer applications, and as they may be used at low temperatures, the noise rise due to chaos may be important. A more complete analysis at $T \neq 0$ for these RSQUIDs configured as mixers with external signal injection will be reported elsewhere.

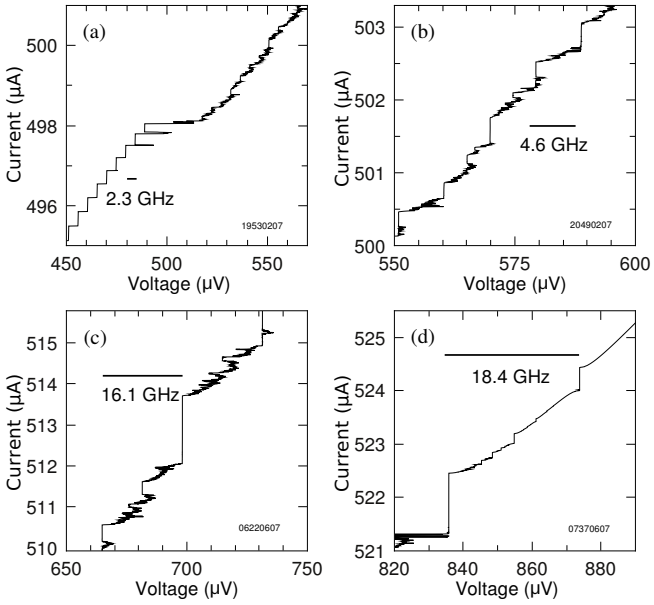

Fig. 8. (a) Onset of chaos at $f_\mathrm{h} = 2.3\,$GHz above $498\,\mu$A, which largely obliterates the steps. (b) At 4.6 GHz some parts of $1/2$-integer steps are visible within the chaotic region of the I-V curve. (c) At 16.1 GHz $1/2$ and $1/4$ steps can be seen. (d) A region at 18.4 GHz showing $1/2$, $1/3$ and $1/4$ steps. The horizontal bars show the voltage $f_\mathrm{h}\Phi_0$. All plots are for $C_\mathrm{J} = 18\,$fF, $R_\mathrm{J} = 8\,\Omega$ and $R_\mathrm{s} = 9.5\,\mathrm{m}\Omega$. f_h is changed by varying I_s.

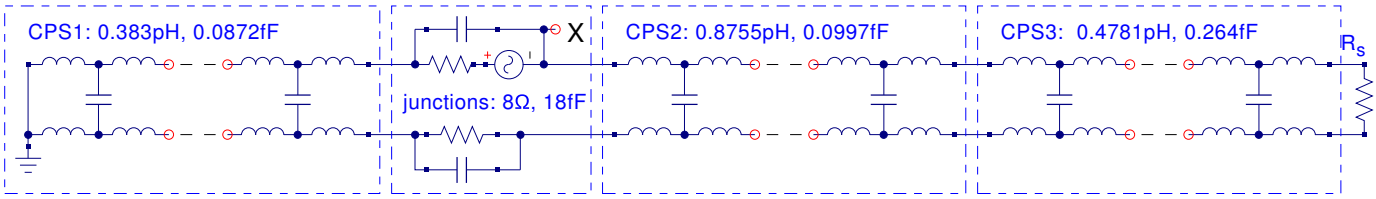

Fig. 9. L-C ladder model of co-planar striplines 1, 2 and 3. The inductance and capacitance values shown are for each element in the ladder, and each CPS has 10 elements. Resistors (not shown) have been added across each capacitor to include the effects of dielectric loss in the MgO, as given in [30]. The voltage source represents the AC Josephson voltage of one junction. Resonances are detected at point X.

VI. A CO-PLANAR TRANSMISSION LINE MODEL

The high I_cR_J product for our RSQUIDs means that they can be biased at 3 mV or more, where the Josephson frequency is $>$ 1 THz. At such frequencies the part of the RSQUID loop not covered by Au in Figs. 2(a) and (c) should be treated as a co-planar stripline (CPS), rather than as a simple lumped inductance. Similar issues have been considered for DC SQUIDs on $SrTiO_3$, where such resonances are at very much lower frequencies, due to the high dielectric constant of $SrTiO_3$ [31]–[33].

We represent the CPS in three parts, as shown in Fig. 10, corresponding to the sections marked CPS 1, 2 and 3 in Fig. 2(c). We expect quarter-wavelength ($\lambda/4$) resonances to be excited in the sections either side of the junctions. R_s is effectively a short-circuit at these resonant frequencies ($>$ 1 THz): its impedance is purely resistive (Fig. 4) and although it is higher than its DC value, it is still much less than any of the CPS line impedances.

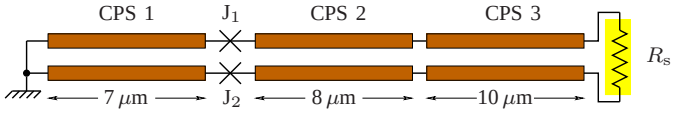

Fig. 10. Simplified CPS model for the RSQUID. The spacing between the tracks is s, their width is w and the line length is ℓ; dimensions are in Table I. J_1 and J_2 are the junctions.

We derived the inductance L_0 and capacitance C_0 per unit length from standard elliptic integral expressions [34] and expressions for kinetic inductance [31]–[33], [35]. The MgO dielectric constant $\epsilon_r = 10$ at ≈ 1 THz [30]. Table I has the data, including the characteristic impedance Z_0 for each part.

TABLE I
PARAMETERS FOR THE CPS RSQUID MODEL SHOWN IN FIG. 10.

CPS	s (μm)	w (μm)	ℓ (μm)	Z_0 (Ω)	L_0 (pH/μm)	$L_0\ell$ (pH)	C_0 (fF/μm)	$C_0\ell$ (fF)
1	4	2	7	132	1.09	7.66	0.062	0.44
2	4	2	8	132	1.09	8.75	0.062	0.50
3	6	50	10	60	0.48	4.78	0.132	1.32

JSIM does not have a balanced 4-port CPS model—its transmission-line model is unbalanced with all of one side at ground potential. So for this structure we followed standard practice and modeled each CPS as an L-C ladder network, We first set up a QUCS circuit, as in Fig. 9, for AC simulation up to 10 THz. Fig. 11 shows the CPS have various $\lambda/4$ resonances. The lowest is at $f_{\lambda/4} = 2.664$ THz.

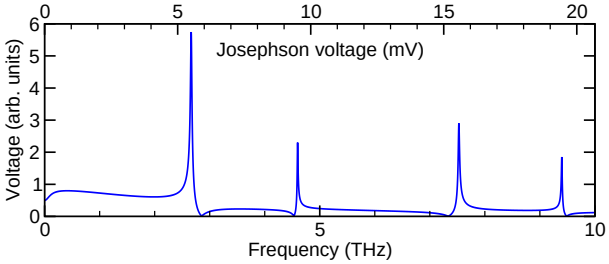

Fig. 11. The AC amplitude at point X in Fig. 9, showing some of the lower $\lambda/4$ resonances. The broad $LC_J/2$ resonance below 1 THz is still present.

The L-C networks for the CPS were then incorporated into a JSIM model. The series resistor was modeled as a pure resistance of $9.5\,\mathrm{m}\Omega$. We find the Josephson frequency, or one of its harmonics, excites this resonance at 2.664 THz. Fig. 12 shows how the fundamental, and also the second and third harmonics excite this resonance and introduce features in the I-V curve. Other fundamental resonances at higher frequencies can also be found.

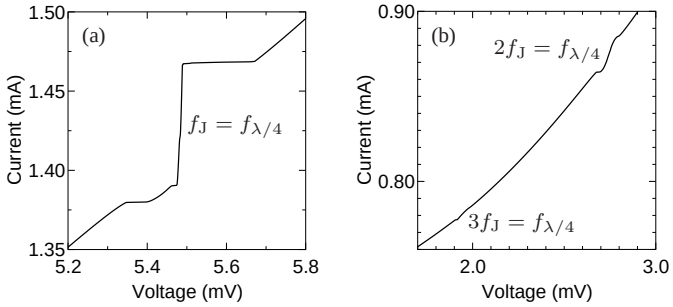

Fig. 12. Excitation of the lowest CPS $\lambda/4$ resonance (a) at the Josephson frequency and (b) by its second and third harmonics.

The CPS model shows that $\lambda/4$ resonances are unlikely to seriously affect our RSQUIDs at frequencies of current interest. However, future designs, which may have additional CPS structures, may need to consider adverse effects of such resonances. But we note that the fundamental resonance markedly changes the slope of the I-V curve and we will study this as a way to potentially enhance the sensitivity of an RSQUID as a tuned mixer or detector.

ACKNOWLEDGMENT

We thank Dr Richard Taylor and Dr Steven Cooper of Mesaplexx Pty, Ltd., Brisbane, Australia, for their expert inputs and Mesaplexx for financial contribution at an earlier stage of this project.

REFERENCES

[1] R. J. Soulen, W. E. Fogle, and J. H. Colwell, "Measurements of absolute temperature below 0.75 K using a Josephson-junction noise thermometer," *J. Low Temp. Phys.*, vol. 94, no. 5, pp. 385–487, Mar. 1994. [Online]. Available: http://dx.doi.org/10.1007/BF00753823

[2] J. G. Park and A. Vaidya, "Resistive SQUIDs for thermal measurements," *IEEE Trans. Magn.*, vol. 17, no. 1, pp. 845–848, Jan. 1981. [Online]. Available: http://ieeexplore.ieee.org/xpls/abs_all.jsp?arnumber=1061120

[3] J. G. Park and A. W. Vaidya, "Resistive SQUID calorimetry at low temperatures," *J. Low Temp. Phys.*, vol. 40, no. 3, pp. 247–274, Aug. 1980. [Online]. Available: http://dx.doi.org/10.1007/BF00117118

[4] G. S. Krivoy and H. Koch, "An all thin-film resistive DC SQUID — a current-controlled oscillator," *Supercond. Sci. Technol.*, vol. 5, no. 10, pp. 605–608, Oct. 1992. [Online]. Available: http://dx.doi.org/10.1088/0953-2048/5/10/009

[5] G. S. Krivoy, C. Aßmann, M. Peters, and H. Koch, "Design and fabrication of thin-film resistive SQUIDs," *J. Low Temp. Phys.*, vol. 99, no. 1, pp. 107–120, Apr. 1995. [Online]. Available: http://dx.doi.org/10.1007/BF00753623

[6] G. S. Krivoy and H. Koch, "Thin-film resistive SQUIDs," *IEEE Trans. Appl. Supercond.*, vol. 5, no. 2, pp. 3244–3247, Jun. 1995. [Online]. Available: http://dx.doi.org/10.1109/77.403283

[7] S. Menkel, C. Aßmann, G. Krivoy, and H. Koch, "An all thin film resistive dc SQUID," *Czech. J. Phys.*, vol. 46, pp. 2863–2864, Apr. 1996. [Online]. Available: http://dx.doi.org/10.1007/BF02570418

[8] S. Menkel, D. Drung, C. Aßmann, and T. Schurig, "A resistive d.c. SQUID noise thermometer," *Appl. Supercond.*, vol. 6, no. 7-9, pp. 417–422, Jul. 1998. [Online]. Available: http://dx.doi.org/10.1016/S0964-1807(98)00109-4

[9] S. Menkel, D. Drung, Y. S. Greenberg, and T. Schurig, "Integrated thin-film dc RSQUIDs for noise thermometry," *J. Low Temp. Phys.*, vol. 120, no. 5, pp. 381–400, Sep. 2000. [Online]. Available: http://dx.doi.org/10.1023/A:1004640804558

[10] S. L. Thomasson and C. M. Gould, "Ultralow temperature SQUIDs for primary thermometry," *IEEE Trans. Appl. Supercond.*, vol. 9, no. 2, pp. 3507–3510, Jun. 1999. [Online]. Available: http://dx.doi.org/10.1109/77.783786

[11] J. C. Macfarlane, L. Hao, D. A. Peden, and J. C. Gallop, "Linewidth of a resistively shunted high-temperature-superconductor Josephson heterodyne oscillator," *Appl. Phys. Lett.*, vol. 76, no. 13, pp. 1752–1754, Mar. 2000. [Online]. Available: http://dx.doi.org/10.1063/1.126156

[12] L. Hao, D. A. Peden, J. C. Gallop, and J. C. Macfarlane, "Tunable HTS rf Josephson-effect oscillator based on YBCO-Au-YBCO resistive SQUID," *Supercond. Sci. Technol.*, vol. 14, no. 12, pp. 1119–1123, Dec. 2001. [Online]. Available: http://dx.doi.org/10.1088/0953-2048/14/12/329

[13] J. Macfarlane, J. Du, R. Taylor, and C. Pegrum, "Simulation and measurement of HTS Josephson heterodyne oscillator," *IEEE Trans. Appl. Supercond.*, vol. 19, no. 3, pp. 920–923, Jun. 2009. [Online]. Available: http://dx.doi.org/10.1109/TASC.2009.2018803

[14] J. Du, J. C. Macfarlane, and L. Hao, "Noise temperature and linewidth of high-temperature-superconducting heterodyne gigahertz oscillators," *Appl. Phys. Lett.*, vol. 93, no. 3, p. 033507, Jul. 2008. [Online]. Available: http://link.aip.org/link/?APL/93/033507/1

[15] J. Du, J. C. Macfarlane, S. H. K. Lam, and R. Taylor, "HTS Josephson heterodyne oscillator on a pulse-tube cryocooler," *Supercond. Sci. Technol.*, vol. 22, no. 10, p. 105013, Oct. 2009. [Online]. Available: http://dx.doi.org/10.1088/0953-2048/22/10/105013

[16] C. M. Pegrum and J. C. Macfarlane, "Self-induced structure in the current-voltage characteristics of RSQUIDs," *IEEE Trans. Appl. Supercond.*, vol. 19, no. 3, pp. 778–781, Jun. 2009. [Online]. Available: http://dx.doi.org/10.1109/TASC.2009.2019591

[17] C. M. Pegrum, "The dynamics of high-frequency DC RSQUID oscillators," *Supercond. Sci. Technol.*, vol. 22, no. 6, p. 064004, Jun. 2009. [Online]. Available: http://stacks.iop.org/0953-2048/22/064004

[18] E. S. Fang and T. Van Duzer, "A Josephson integrated circuit simulator (JSIM) for superconductive electronics application," in *Extended abstracts of the Int. Supercond. Electronics Conf. (ISEC'89), Tokyo, Japan*, 1989, pp. 407–410. [Online]. Available: http://www-cryo.eecs.berkeley.edu/software/JSIM_ISEC89.pdf

[19] J. Satchell, "Stochastic simulation of SFQ logic," *IEEE Trans. Appl. Supercond.*, vol. 2, no. 7, pp. 3315–3318, Jun. 1997. [Online]. Available: http://dx.doi.org/10.1109/77.622070

[20] C. M. Pegrum, "Control programs to generate I-V and V-Φ curves," in *Extended abstracts of the Int. Supercond. Electronics Conf. (ISEC'97), Berlin, Germany*, 1997, pp. 34–36. [Online]. Available: http://fsolv.co.uk/pegrum-34.pdf

[21] J. Du, A. D. Hellicar, L. Li, S. M. Hanham, J. C. Macfarlane, K. E. Leslie, N. Nikolic, C. P. Foley, and K. J. Greene, "Terahertz imaging at 77K," *Supercond. Sci. Technol.*, vol. 22, no. 11, p. 114001, Nov. 2009. [Online]. Available: http://stacks.iop.org/0953-2048/22/i=11/a=114001

[22] C. M. Pegrum, "RSQUID modelling and design," Feb. 2009, technical report, unpublished.

[23] W. H. Chang, "Numerical calculation of the inductances of a multi-superconductor transmission line system," *IEEE Trans. Magn.*, vol. MAG-17, pp. 764–766, Jan. 1981. [Online]. Available: http://dx.doi.org/10.1109/TMAG.1981.1060982

[24] QUCS: Quite Universal Circuit Simulator, v. 0.0.15. [Online]. Available: http://qucs.sourceforge.net

[25] Fasthenry is available from Whiteley Research Inc., 456 Flora Vista Avenue, Sunnyvale, CA 94086 USA. [Online]. Available: http://wrcad.com/freestuff.html

[26] H. Töpfer, G. Mäder, and H. Uhlmann, "Accurate calculation of capacitances of grain boundary Josephson junctions in high critical temperature superconductors," *J. Appl. Phys.*, vol. 77, no. 9, pp. 4576–4579, May 1995. [Online]. Available: http://link.aip.org/link/?JAP/77/4576/1

[27] J. Du, A. D. Hellicar, L. Li, S. M. Hanham, N. Nikolic, J. C. Macfarlane, and K. E. Leslie, "Terahertz imaging using a high-T_c superconducting Josephson junction detector," *Supercond. Sci. Technol.*, vol. 21, no. 12, p. 125025, Dec. 2008. [Online]. Available: http://stacks.iop.org/0953-2048/21/i=12/a=125025

[28] E. E. Mitchell and C. P. Foley, "YBCO step-edge junctions with high $I_c R_n$," *Supercond. Sci. Technol.*, vol. 23, no. 6, p. 065007, Jun. 2010. [Online]. Available: http://stacks.iop.org/0953-2048/23/i=6/a=065007

[29] E. Ott, *Chaos in dynamical systems*. Cambridge and New York: Cambridge University Press, 1993, pp. 6–8.

[30] T. Kiwa and M. Tonouchi, "Time-domain terahertz spectroscopy of (100) $(LaAlO_3)_{0.3}$-$(Sr_2AlTaO_6)_{0.7}$ substrate," *Jpn. J. Appl. Phys.*, vol. 40, Part 2, no. 1A/B, pp. L38–L40, Jan. 2001. [Online]. Available: http://jjap.ipap.jp/link?JJAP/40/L38/

[31] K. Enpuku, T. Maruo, and T. Minotani, "Effect of large dielectric constant of $SrTiO_3$ substrate on the characteristics of high T_c dc superconducting quantum interference device," *J. Appl. Phys.*, vol. 80, no. 2, pp. 1207–1213, Jul. 1996. [Online]. Available: http://dx.doi.org/10.1063/1.362858

[32] U. Sinha, A. Sinha, and E. J. Tarte, "On transmission line resonances in high T_c dc SQUIDs," *Supercond. Sci. Technol.*, vol. 21, no. 8, p. 085021, Aug. 2008. [Online]. Available: http://dx.doi.org/10.1088/0953-2048/21/8/085021

[33] U. Sinha, A. Sinha, and F. K. Wilhelm, "Improving high-T_c dc SQUID performance by means of junction asymmetry," *Supercond. Sci. Technol.*, vol. 22, no. 5, p. 055002, May 2009. [Online]. Available: http://dx.doi.org/10.1088/0953-2048/22/5/055002

[34] R. Simons, *Coplanar waveguide circuits, components, and systems*. New York: John Wiley, 2001, pp. 152–156.

[35] K. Yoshida, M. S. Hossain, T. Kisu, K. Enpuku, and K. Yamafuji, "Modeling of kinetic-inductance coplanar stripline with NbN thin-films," *Jpn. J. Appl. Phys.*, vol. 31, Part 1, no. 12A, pp. 3844–3850, Dec. 1992. [Online]. Available: http://dx.doi.org/10.1143/JJAP.31.3844